

Online Phase and Amplitude Distortion Compensation in FOPA Transmission Systems

Long H. Nguyen, Sonia Boscolo, and Stylianos Sygletos

Aston Institute of Photonic Technologies, Aston University, Birmingham B4 7ET, United Kingdom
{lnguy19, s.a.boscolo, s.sygletos}@aston.ac.uk

Abstract: We present an online digital signal processing scheme for compensating the phase and amplitude distortions induced by the pump phase modulation and its interaction with the dispersive fibre channel in fibre-optical parametric amplified transmission systems.

© 2024 The Author(s)

1. Introduction

Today mitigating stimulated Brillouin scattering (SBS) remains a significant challenge for the eventual penetration of fibre-optical parametric amplifiers (FOPAs) into future communication systems [1]. The SBS effect limits the pump power that can be delivered to the highly nonlinear fibre (HNLF), and thereby the achievable nonlinear phase shift. The phase modulation that is commonly used to broaden the line-width of the pump source so to minimise the power spectral density integrated over the Brillouin bandwidth [2], causes temporal variation of the parametric gain [3], which is primarily a source of phase distortion for coherently detected complex-amplitude signals [4]. Having a relatively high frequency, this phase distortion can not be tracked and sufficiently suppressed by the conventional carrier phase recovery (CPR) schemes [5] deployed in commercial coherent receivers.

Recently, we have developed a number of digital signal processing (DSP) techniques that can effectively address the impact of phase distortion caused by pump dithering in fibre-optical parametric devices [6, 7]. In [7], we presented a scheme that can mitigate the intrinsic dithering-induced phase distortion and its conversion into amplitude distortion when interacting with the fibre dispersion in transmission links with mid-span optical phase conjugation. This paper extends the approach of [7] to transmission links with cascaded in-line FOPAs, operating with multi-tone pump dithering to support sufficient SBS-limited gain. We introduce a fully online DSP scheme enabling the removal of the accumulated phase and amplitude distortions that are independently contributed by each FOPA stage in the link. The technique is numerically demonstrated in 28-Gbaud 16 quadrature amplitude modulation (QAM) transmission, achieving significant Q^2 -factor improvement over conventional DSP.

2. Methods, Results, and Discussion

We considered a transmission system comprising N identical spans, each of 100-km standard single-mode fibre (dispersion parameter $D = 17 \text{ ps}/(\text{nm} \cdot \text{km})$, loss coefficient $\alpha = 0.2 \text{ dB/km}$, nonlinear coefficient $\gamma' = 1.2 (\text{W} \cdot \text{km})^{-1}$) followed by a FOPA to compensate the propagation losses. In our model of the FOPA, we used a single-pump design and calculated the signal gain in the absence of pump depletion as in [8], where the phase mismatch comprised an additional instantaneous term induced by the phase modulation of the pump, $\varphi(t)$, following [3]. We operated the FOPA at its maximum power gain of 25 dB, where this gain value was chosen to account for typical device's insertion losses. Given that the Kerr-to-Brillouin figure of merit $\gamma P_{\text{th}} L$ (L is the effective length, and P_{th} is the SBS power threshold) is in the range 0.2 to 0.3 rad for a range of HNLFs in the 1550-nm region [1], reaching a gain level of 25 dB requires an SBS threshold enhancement of at least 12 dB. This was achieved through a suitably designed multi-tone modulation of the pump phase. We considered 3- and 4-tone phase modulations, $\varphi(t) = \sum_{j=1}^{N_t} A_{mj} \sin(\omega_{mj} t + \xi_{mj})$, $N_t = 3$ or 4, with the $N_t = 3$ scheme representing a viable, yet rather marginal choice. The base modulation frequency was $\nu_{m1} = 100 \text{ MHz}$, and we chose a multiple of 3 spacing between subsequent tones to maximise the pump spectral broadening and power distribution [9]. The amplitudes A_{mj} and phases ξ_{mj} of the tones were optimised to even out the power distribution among the 3^{N_t} peaks generated across the broadened pump spectrum by implementing a stochastic gradient descent method in TensorFlow.

To derive the proposed dithering distortion compensation (DDC) algorithm, we assumed the equivalent base-band model of Fig. 1(a) (amplified spontaneous emission noise addition not shown), where $h_f(t)$ represents the linear impulse response of each fibre span, $\phi_t(t)$ and $\phi_r(t)$ are the Wiener random phase noises (PNs) of the transmitter and receiver laser sources, respectively (50-kHz line-widths), $\Psi^{(n)}(t) = \phi_p^{(n)}(t) + \phi^{(n)}(t)$ is the phase noise introduced at the n th FOPA stage, $\phi_p^{(n)}(t)$ is the pump laser PN (30-kHz line-width), and $\phi^{(n)}(t)$ represents the dithering-induced phase distortion. By applying linear back-propagation to the relationship between input $x(t)$ and output $y(t)$ signal wave-forms, we derived an approximate estimate of the transmitted signal $\hat{x}(t)$. This equation evidenced that the output signal from a conventional DSP chain including chromatic dispersion compensation (CDC) and CPR, $y'(t) = e^{-i\delta\phi(t)} [y(t) * h_e^{(N)}(t)]$ (where $\delta\phi(t) = \sum_n \phi_p^{(n)}(t) + \phi_t(t) + \phi_r(t)$, and $h_e(t)$ the inverse response of the fibre span), differs from the transmitted signal by an additional dithering-dependent

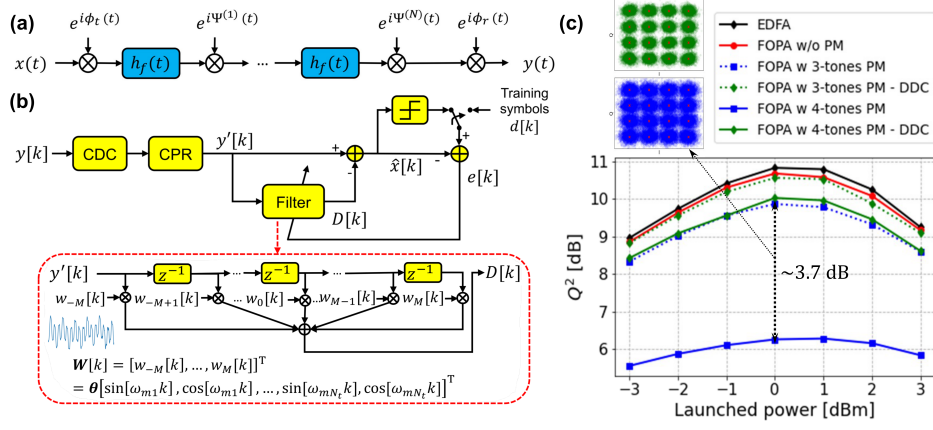


Fig. 1. (a) Base-band equivalent of the FOPA link. (b) Block diagram of the proposed DDC-enabled DSP chain. The inset shows the principle of the DDC algorithm. (c) Q^2 -factor after conventional (CDC+CPR) DSP (blue) and the proposed DDC (green) versus launched signal power after 10 fibre spans for 3-tone (dotted) and 4-tone (solid) pump phase modulations. The inset shows the constellation diagrams at the optimum launched power. The performance curves for in-line EDFAs (black) and dithering-free FOPAs (red) are also shown.

complex distortion term, which becomes more important with increasing number of fibre spans. By approximating the channel impulse response by a finite impulse response filter, this distortion term at the time instance k can be written as $D[k] = i \sum_{m,m'=-M/2}^{M/2} y'[k-m-m'] \sum_{n=1}^N (h_{f,m}^{(n)} \phi^{(n)}[k-m'] h_{e,m'}^{(n)})$, where $M/2$ is the filter delay corresponding to the channel memory of the N -span link. This equation shows that we can recreate $D[k]$ by passing $y'[k]$ through an adaptive digital filter whose taps have similar form to the first-order time derivative of the pump phase ϕ_i (inset of Fig. 1(b)) and, thus, can be predicted by fitting a parametric model with the known pump phase modulation frequencies used at each FOPA stage. Therefore, by using the complex least-mean-square algorithm [10], we fitted a time-varying filter $\mathbf{W}[k] = [w_{-M}[k], \dots, w_M[k]]^T$ such that $D[k] = \mathbf{W}^T[k] \mathbf{Y}'[k]$, where $\mathbf{Y}'[k]$ represents the signal block after the conventional CDC and CPR stages. The filter was trained by updating the coefficient vector $\boldsymbol{\theta}$ in the linear regression form $\mathbf{W} = \boldsymbol{\theta} \mathbf{B}$, where the feature vector was defined as $\mathbf{B}[k] = [\sin[\omega_{m1}k], \cos[\omega_{m1}k], \dots, \sin[\omega_{mN_i}k], \cos[\omega_{mN_i}k]]^T$. The transmitted signal at time k was then recovered as $\hat{x}[k] = y'[k] - \mathbf{W}^T[k] \mathbf{Y}'[k] = y'[k] - \mathbf{B}^T \boldsymbol{\theta} \mathbf{Y}'[k]$. We updated $\boldsymbol{\theta}$ at the symbol rate using the error calculated from the estimated symbol and the reference one, where the reference symbol was given from the decision-directed operation when the algorithm exited the training phase.

We simulated the transmission of a 28-Gbaud 16 quadrature-amplitude modulation Nyquist-shaped signal with a roll-off factor of 0.1 and 8 samples per symbol. A random phase fluctuation was introduced at each FOPA stage. We used the Q^2 -factor derived from the direct-count bit-error-rate (BER) on a total number of 10×2^{16} symbols as a performance metric. Figure 1(c) shows the performance of the proposed DDC algorithm as a function of the launched signal power after 8 fibre spans. The lengths of the blind-phase search filter used for CPR [5] and of the DDC filter were optimised for each power. We also included the performance curves of transmission links with in-line erbium-doped fibre amplifiers (EDFAs) and pump-dithering-free FOPAs as a reference. The amplifier's gain and noise figure were 25 dB and 4.5 dB, respectively, in all cases. The EDFA amplification obviously represents the best scenario, while the transmission scheme with dithering-free FOPAs performs slightly worse due to the presence of pump laser PN. With the 3-tone dithering FOPA scheme, our DDC method achieves almost 1-dB Q^2 improvement over conventional DSP and shows similar performance to the dithering-free FOPA scheme. In the 4-tone dithering case, the algorithm brings about significant performance benefits, achieving ~ 3.7 -dB Q^2 improvement at the (optimum) powers in the range 0-1 dBm, where the BER after conventional DSP is 2×10^{-2} .

3. Conclusion

We presented an online DSP scheme to tackle the phase and amplitude distortions originating from the pump dithering and its interaction with the fibre dispersion in transmission systems with cascaded FOPAs. We believe that our scheme may become a key component in future FOPA-based links, where pump dithering will be necessary to achieve high amplification gains. **Acknowledgements:** We acknowledge support from the H2020 MSCA programme (EC GA 860360), the UK EPSRC (EP/R035342/1, EP/X019241/1) and RAEng (RCSR fellowship).

References

1. V. Gordienko *et al.*, Opt. Fiber Technol. **66**, 102646 (2021).
2. J.B. Coles *et al.*, Opt. Express **18**, 18138–18150 (2010).
3. A. Mussot *et al.*, IEEE Photon. Technol. Lett. **16**, 1289–1291 (2004).
4. M. Bastamova *et al.*, Proc. ECOC 2022, Tu5.6.
5. T. Pfau *et al.*, J. Lightwave Technol. **27**, 989–999 (2009).
6. S. Boscolo *et al.*, Opt. Express **30**, 19479–19493 (2022).
7. L.H. Nguyen *et al.*, Proc. CLEO 2023, SM3I.5.
8. M.E. Marhic, *Fiber Optical Parametric Amplifiers, Oscillators and Related Devices* (Cambridge Univ. Press, 2007).
9. S.K. Korotky *et al.*, Proc. CIOOFC 1995, 110–111.
10. B. Widrow *et al.*, IEEE Proc. **63**, 719–720 (1975).